An ankle rehabilitation robot based on 3-RRS spherical parallel mechanism

Du, Yuting; Li, Ruiqin; Li, Dahai; Bai, Shaoping

Published in:
Advances in Mechanical Engineering

DOI (link to publication from Publisher):
10.1177/1687814017718112

Publication date:
2017

Document Version
Publisher's PDF, also known as Version of record

Research Article

Advances in Mechanical Engineering

Advances in Mechanical Engineering
2017, Vol. 9(8) 1–8

DOI: 10.1177/1687814017718112
journals.sagepub.com/home/ade
SAGE

An ankle rehabilitation robot based on 3-RRS spherical parallel mechanism

Yuting Du[1], Ruiqin Li[1], Dahai Li[1] and Shaoping Bai[2]

Abstract

This article presents the design modeling of a novel 3-RRS spherical parallel mechanism for ankle rehabilitation applications. The kinematics of the 3-RRS spherical parallel mechanism is established. The degree of freedom of 3-RRS spherical parallel mechanism is calculated using screw theory. The inverse kinematics of 3-RRS spherical parallel mechanism is solved. Eight groups of inverse solutions of 3-RRS spherical parallel mechanism are obtained. A method for forward position analysis is developed with variation and iteration approaches, which is suitable for motor position control. The ankle rehabilitation robot can be widely used in clinical treatment and can also be used at home, hotels, and fitness centers for ankle muscle relaxation.

Keywords

3-RRS, spherical parallel mechanism, forward position analysis, inverse position analysis, ankle rehabilitation robot

Date received: 6 February 2017; accepted: 31 May 2017

Academic Editor: Soheil Salahshour

Introduction

Ankle sprain is one of the common sport injuries, particularly in complex movement such as in the ball games, where there are sudden changes in direction, or urgent start and stop bring in the problems.[1] If the injuries are not treated timely or thoroughly, it can lead to ankle ligament laxity and joint instability and cause repeated injuries. In the worst cases, it can lead to more serious problems such as ankle dysfunctions.

The development of robot technology makes possible to perform ankle rehabilitation effectively with a robotic device. An ankle rehabilitation robot can not only reduce the labor intensity of the doctor but also can quantitatively evaluate patient rehabilitation condition. The robots make them possible for regularly, moderately rehabilitation exercises.

Some ankle rehabilitation robots in experimental study or the market products have been reported in the literature. A 2-RRR/UPRR (R-revolute joint, U-universal joint, P-prismatic joint) robot mechanism for ankle rehabilitation is presented by Bian et al.,[2] where the mechanism can realize three rotations around the remote center and satisfy the requirements of ankle rehabilitation motions. Wang et al.[3] presented a novel parallel ankle rehabilitation robot and achieved the kinematic solution and simulation analysis. A parallel robot for ankle rehabilitation was reported by Shah and Basah.[4] Hou et al.[5] proposed a concept of ankle rehabilitation mechanism, which can train the movements of flexion, inversion, and eversion of ankle. A decoupled parallel mechanism designed for ankle

[1]School of Mechanical Engineering, North University of China, Taiyuan, China
[2]Department of Mechanical and Manufacturing Engineering, Aalborg University, Aalborg, Denmark

Corresponding author:
Ruiqin Li, School of Mechanical Engineering, North University of China, Taiyuan 030051, China.
Email: liruiqin@nuc.edu.cn

rehabilitation is presented by Zeng et al.;[6] the proposed mechanism can realize independent rotational rehabilitation under the traction simultaneously. Other parallel ankle rehabilitation robots can be found in Jamwal et al.,[7] Dai, et al.,[8] Girone, et al.,[9] Zhao, et al.,[10] among others.

It can be noted that the existing ankle rehabilitation robots have some limitations. First, most robots have only 1 or 2 degrees of freedom (DOFs) and cannot be used for comprehensive rehabilitations in all degrees of angle motions. Second, for most robots, their rotation centers can easily shift away from the rotation center of human ankle. Such a shift can cause uncomfortable feeling in the patients, or in the worst case cause secondary injury of ankle joint. An ankle rehabilitation robot with simple structure, which can fully meet the ankle structure characteristics and realize ankle rehabilitation motion, is needed.

In this work, we propose a spherical parallel manipulator for ankle rehabilitations. The robot is based on a 3-revolute–revolute–spherical joint's (RRS) spherical parallel mechanism (SPM), which generates rotation analogy to human ankles.

The motion of human ankle

Prior to the design of the SPM, we looked at the biomechanics of human ankle motion to determine robot specifications properly.

Movement of human ankle joint

As shown in Figure 1, ankle joint has three kinds of movements: dorsiflexion and plantar flexion, inversion and eversion, adduction and abduction.

The ranges of motion of ankle joint are shown in Table 1.

The motion curve of foot relative to ankle

Based on the anthropometric measurements,[14] the distance between the moving center of the ankle and the bottom of the foot is generally 60–100 mm long. The size of the foot is 210–270 mm long for 96% female over the age of 14 and 240–285 mm long for 96% male over the age of 15.

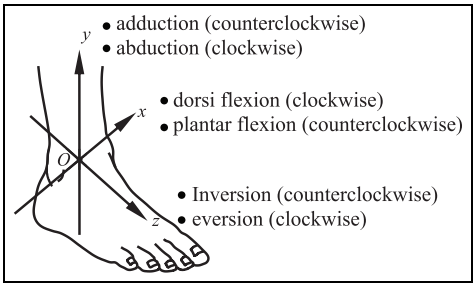

Figure 1. The motion of human ankle joint.

In Figure 2, the distance between the moving center O of the ankle and the bottom of the foot B takes as 80 mm. The distance between the moving center O of the ankle and the front of foot A takes a value of 240 mm. Taking this foot size as an example, we analyze the motion curve of the foot relative to ankle.

The moving center O of the ankle is as the coordinate origin. The motion curve of the front of foot A relative to moving center O of the ankle based on the coordinate system in Figure 1 is shown in Figure 3.

The 3-RRS SPM for ankle rehabilitation

The conceptual design of the 3-RRS rehabilitation robot is shown in Figure 4, which includes the base, the moving platform, support, motor, crank, coupler, foot support, expansion device, and so on. Three motors drive the cranks to generate the rotations of the moving platform around the center of the sphere.

The adjustable length of the expansion device is 50 mm, which can be applied to most patients. Compared with the existing ankle rehabilitation robots, the ankle rehabilitation robot based on 3-RRS SPM mainly shows some unique features as follows:

Table 1. The range of motion of ankle joint.

Rotation direction	Name	Human limit swing angle (°)	Human normal walking angle (°)[a]	Angle of mechanism design (°)[b]
CW around *x*-axis	Dorsiflexion	0–20 (30)[c]	0–14	0–20
CCW around *x*-axis	Plantar flexion	0–30 (50)[c]	0–20	0–25
CCW around *z*-axis	Inversion	0–30[d]	0–14	0–20
CW around *z*-axis	Eversion	0–15[d]	0–10	0–15
CCW around *y*-axis	Adduction	0–30[e]	0–25	0–30
CW around *y*-axis	Abduction	0–35[e]	0–25	0–30

CW: clockwise; CCW: counterclockwise.

[a]The data are taken from the Yao Taishun's book *Ankle Surgery*.[13]

[b]The data are the design parameters in this article.

[c]The data are taken from the third chapter in Kapandji's book *The Ankle*.[11] The numbers in parentheses indicate the difference among individuals.

[d]The data are taken from the 18th chapter in Dror Paley's book *Principles of deformity correction*.[12]

[e]The data are taken from the David's book *Foot & ankle*.[1]

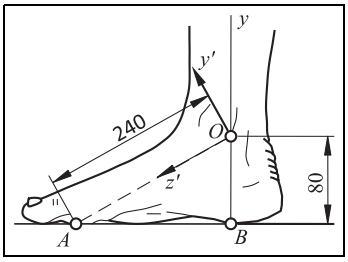

Figure 2. The sizes of the foot.

1. The mechanism can implement 3-DOF rotation to be completely compatible for human ankle motion.
2. The mechanism is adjustable and controllable by adjusting the telescopic rod in the expansion device to adapt to the different sizes of feet.
3. The location of the spherical center O of 3-RRS SPM remains during movement. On the other hand, the center position can be adjusted according to the distance between ankle movement center and the bottom of foot adjusting the telescopic rod of the mechanism, to make the ankle movement center coincide with the spherical center.
4. The mechanism has a large range of motion in its three axes. This allows the magnitude of rotation adjustable to satisfy the requirements of different rehabilitations.

Kinematics of 3-RRS SPM

Kinematic parameters and coordinate systems of 3-RRS SPM

Figure 5 shows the kinematics model of 3-RRS SPM. It is composed of the base, the crank, the coupler, and the moving platform. It has three limbs with identical structures.

In each limb, there are two revolute pairs R and one spherical pair S. The point O represents spherical center. The point P represents the geometrical center of the moving platform. The point G represents the geometrical center of the base. A_i, B_i, and C_i represent the center of the kinematic pair in limb i ($i = 1, 2, 3$), respectively.

The structure parameters of 3-RRS SPM are shown in Table 2. The cone angles φ_1 and φ_2 of the moving platform and the base are 54.74°. Three axes OA_1, OA_2, and OA_3 of the revolute joints connecting the cranks and the base are perpendicular to each other in space and intersect at the spherical center. Three lines OC_1, OC_2, and OC_3 between the centers C_i ($i = 1, 2, 3$) of the spherical pairs and the spherical center O are perpendicular to each other in space.

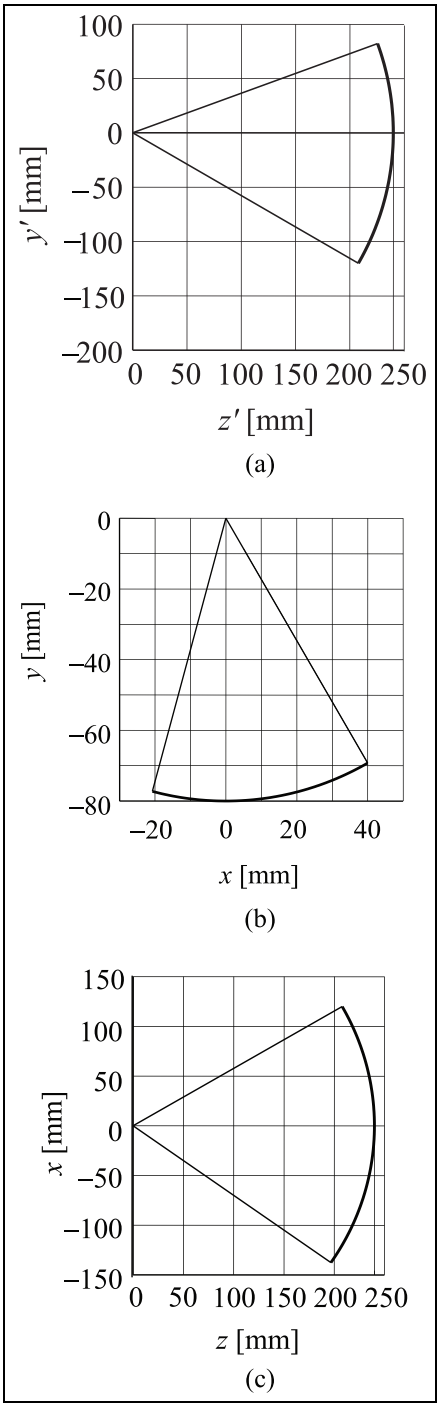

Figure 3. The movement curves of foot with respect to ankle: (a) the curve of dorsiflexion and plantar flexion, (b) the curve of inversion and eversion and (c) the curve of adduction and abduction.

The fixed coordinate system O-XYZ is established at the base. The coordinate origin O is located at the spherical center. The OX, OY, and OZ axes coincide with OA_1, OA_2, and OA_3, respectively.

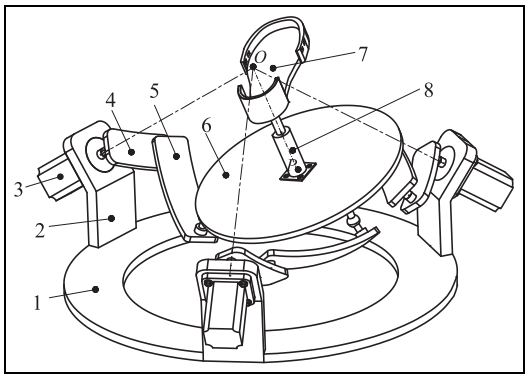

Figure 4. The 3-RRS SPM for ankle rehabilitation.
1: base; 2: support; 3: motor; 4: crank; 5: coupler; 6: moving platform; 7: foot support; 8: expansion device.

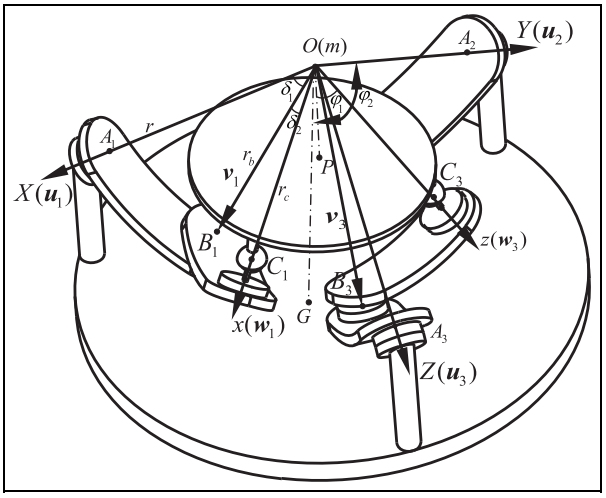

Figure 5. The structure parameters of 3-RRS SPM.

The moving coordinate system *m-xyz* is attached to the moving platform. The coordinate origin *m* is also located at the spherical center *O*. The *mz, mx*, and *my* axes coincide with OC_1, OC_2, and OC_3, respectively.

The kinematic modeling of 3-RRS SPMs is well-documented based on constraint equations of spherical linkages.[15,16] In this work, we develop their model with a different approach.

The DOF calculation of 3-RRS SPM

Figure 6 shows one limb of the 3-RRS SPM. One spherical pair can be seen as three revolute pairs that are concurrent but not coplanar. The axes of six revolute pairs in three limbs intersect at the spherical center *O* of 3-RRS SPM. Based on the principle that the inverse proportion of screw is independent to the choice of coordinate system, taking limb 1 as an example, the kinematic screw system of limb 1 in the *m-xyz* system is

$$\begin{cases} \$_{11} = (a_{11} \quad b_{11} \quad b_{11}; 0 \quad 0 \quad 0) \\ \$_{12} = (a_{12} \quad b_{12} \quad c_{12}; 0 \quad 0 \quad 0) \\ \$_{13} = (1 \quad 0 \quad 0; 0 \quad 0 \quad 0) \\ \$_{14} = (0 \quad b_{14} \quad c_{14}; d \quad 0 \quad 0) \\ \$_{15} = (0 \quad b_{15} \quad c_{15}; d \quad 0 \quad 0) \end{cases} \tag{1}$$

In limb 1, $\$_{11}$, $\$_{12}$, and $\$_{13}$ in different planes intersect one point in space. $\$_{14}$, $\$_{15}$, and $\$_{13}$ are perpendicular to each other in space. Thus, $\$_{11}$, $\$_{12}$, $\$_{13}$, $\$_{14}$, and $\$_{15}$ are linearly independent. The reciprocal basis screw in limb 1 is as follows

$$\begin{cases} \$^r_{11} = (1 \quad 0 \quad 0; 0 \quad 0 \quad 0) \\ \$^r_{12} = (0 \quad 1 \quad 0; 0 \quad 0 \quad 0) \\ \$^r_{13} = (0 \quad 0 \quad 1; 0 \quad 0 \quad 0) \end{cases} \tag{2}$$

According to the relationship between force screw and kinematics screw, limb 1 is subjected to the action of three forces from the axes *X, Y*, and *Z*, not subjected to the action of the couple.

From the structure in Figure 5, the spherical pair S in each limb degenerates into the revolute pair R. Thus, there are two passive DOFs in each limb. The DOF of 3-RRS SPM is calculated as follows using the modified Grübler–Kutzbach equation

$$\begin{aligned} M &= d(n-g-1) + \sum_{i=1}^{g} f_i - \upsilon - \zeta \\ &= 3(8-9-1) + 15 - 0 - 6 = 3 \end{aligned} \tag{3}$$

where *d* is the order of the mechanism, *n* is the link numbers including the frame, *g* is the number of kinematic pairs, f_i is the DOF of *i*th kinematic pair, υ is the number of redundant constraints, and ζ is the number of passive DOFs.

The forward kinematic analysis of 3-RRS SPM

The forward position solution of 3-RRS SPM is to solve the orientation of the moving platform (α, β, γ) for the given three driving angles (θ_1, θ_2, θ_3).

As shown in Figure 5, the position of each kinematic pair axis is represented by unit vector $\boldsymbol{u}_i, \boldsymbol{v}_i, \boldsymbol{w}_i$ in limb *i* (i = 1, 2, 3), respectively. The direction of each kinematic pair axis is pointing from the spherical center *O* to the corresponding kinematic pair center.

In the 3-RRS SPM, the unit vectors $\boldsymbol{u}_1, \boldsymbol{u}_2, \boldsymbol{u}_3$ coincide with *OX, OY*, and *OZ* in the base coordinate system *O-XYZ*, respectively. The unit vectors $\boldsymbol{w}_1, \boldsymbol{w}_2, \boldsymbol{w}_3$ coincide with *mx*, *my*, and *mz* in the moving coordinate system *m-xyz*, respectively. $\boldsymbol{v}_1, \boldsymbol{v}_2, \boldsymbol{v}_3$ coincide with OB_1, OB_2, and OB_3, respectively.

When *Z–Y–X* Euler angles (α, β, γ) are used to represent the orientation of the moving coordinate system *m-xyz* relative to the base coordinate system *O-XYZ*, the transformation matrix $\boldsymbol{R}^m_b$ of *m-xyz* system relative

Table 2. The structure parameters of 3-RRS SPM.

Parameters	Explanation (i = 1, 2, 3)
δ_1	Dimension of curved link A_iB_i
δ_2	Dimension of curved link B_iC_i
φ_1	Cone angle of the moving platform $\angle C_iOP$
φ_2	Cone angles of the base $\angle A_iOG$
r	Radius of the curved link A_iB_i
r_b	Radius of the curved link B_iC_i
r_c	Distance OC_i between the spherical center O and the spherical joint center C_i
h_1	Thickness of the crank and the coupler
h_2	Height of the small boss on the crank and the coupler
l_s	Distance between the spherical joint center and the coupler boss; distance between the spherical joint center and the moving platform

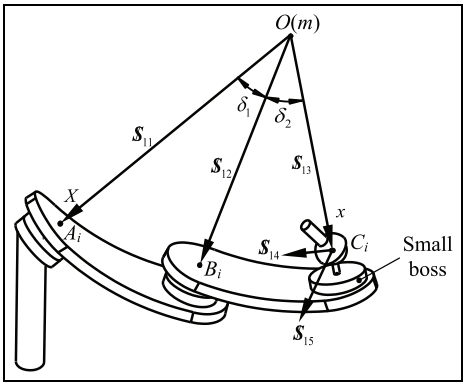

Figure 6. The ith limb of 3-RRS SPM.

to O-XYZ system, based on the exponential product and the Rodrigues' formula, can be expressed as

$$\boldsymbol{R}_b^m = \boldsymbol{e}^{\hat{\boldsymbol{z}}\alpha}\boldsymbol{e}^{\hat{\boldsymbol{y}}\beta}\boldsymbol{e}^{\hat{\boldsymbol{x}}\gamma} \tag{4}$$

Equation (4) can be expanded as

$$\boldsymbol{R}_b^m = \begin{bmatrix} c\alpha c\beta & c\alpha s\beta s\gamma - s\alpha c\gamma & c\alpha s\beta c\gamma + s\alpha s\gamma \\ s\alpha c\beta & s\alpha s\beta s\gamma + c\alpha c\gamma & s\alpha s\beta c\gamma - c\alpha s\gamma \\ -s\beta & c\beta s\gamma & c\beta c\gamma \end{bmatrix}$$

Here and hereafter $c =$ cos and $s =$ sin.

When 3-RRS SPM is in the initial position, the coordinates of the unit vectors $\boldsymbol{u}_i, \boldsymbol{v}_i, \boldsymbol{w}_i$ (i = 1, 2, 3) in the O-XYZ system are

$$\begin{bmatrix} \boldsymbol{u}_{1O} \\ \boldsymbol{u}_{2O} \\ \boldsymbol{u}_{3O} \end{bmatrix} = \begin{bmatrix} 1 & 0 & 0 \\ 0 & 1 & 0 \\ 0 & 0 & 1 \end{bmatrix}, \begin{bmatrix} \boldsymbol{v}_{1O} \\ \boldsymbol{v}_{2O} \\ \boldsymbol{v}_{3O} \end{bmatrix} = \begin{bmatrix} c\delta_1 & s\delta_1 s\theta_1 & s\delta_1 c\theta_1 \\ s\delta_1 c\theta_2 & c\delta_1 & s\delta_1 s\theta_2 \\ s\delta_1 s\theta_3 & s\delta_1 c\theta_3 & c\delta_1 \end{bmatrix}, \begin{bmatrix} \boldsymbol{w}_{1O} \\ \boldsymbol{w}_{2O} \\ \boldsymbol{w}_{3O} \end{bmatrix}$$
$$= \begin{bmatrix} c(\delta_1-\delta_2) & s(\delta_1-\delta_2)s(\pi-\theta_1) & s(\delta_1-\delta_2)c(\pi-\theta_1) \\ s(\delta_1-\delta_2)c(\pi-\theta_2) & c(\delta_1-\delta_2) & s(\delta_1-\delta_2)s(\pi-\theta_2) \\ s(\delta_1-\delta_2)s(\pi-\theta_3) & s(\delta_1-\delta_2)c(\pi-\theta_3) & c(\delta_1-\delta_2) \end{bmatrix}. \tag{5}$$

Suppose the center of three spherical pairs C_i (i = 1, 2, 3) connected the coupler and the moving platforms are all located on the unit sphere, the coordinate of C_i (i = 1, 2, 3) in the O-XYZ system, based on the exponential product and the Rodrigues' formula, can be expressed as

$$\boldsymbol{C}_i(\theta_i) = \boldsymbol{e}^{\hat{\boldsymbol{u}}_{iO}\theta_i}\boldsymbol{e}^{\hat{\boldsymbol{v}}_{iO}\eta_i}\boldsymbol{w}_{iO} \tag{6}$$

where η_i (i = 1, 2, 3) is the angle between links A_iB_i and B_iC_i, called passive angle

$$\boldsymbol{e}^{\hat{\boldsymbol{u}}_{iO}\theta_i} = \boldsymbol{I} + \hat{\boldsymbol{u}}_{iO}\sin\theta_i + (\hat{\boldsymbol{u}}_{iO})^2(1 - cos\ \theta_i);$$
$$\hat{\boldsymbol{u}}_{iO} = \begin{bmatrix} 1 & -u_{iO3} & u_{iO2} \\ -u_{iO3} & 0 & -u_{iO1} \\ -u_{iO2} & u_{iO1} & 0 \end{bmatrix}.$$

In the 3-RRS SPM, the following equation always holds

$$\left\|C_1C_2\right\|^2 = (C_2 - C_1)^{\mathrm{T}}(C_2 - C_1) \tag{7}$$

Differentiating and simplifying equation (7) yield

$$d\left\|C_1C_2\right\| = \frac{(C_2 - C_1)^{\mathrm{T}}}{\left\|\overline{C_1C_2}\right\|}(dC_2 - dC_1) \tag{8}$$

From equation (6), the following expression can be obtained

$$d\boldsymbol{C}_i = \boldsymbol{e}^{\hat{\boldsymbol{u}}_{iO}\theta_i}\boldsymbol{e}^{\hat{\boldsymbol{v}}_{iO}\eta_i}\hat{\boldsymbol{v}}_{iO}\boldsymbol{w}_{iO}d\boldsymbol{\eta}_i \tag{9}$$

Let the distance between point C_1 and point C_2 be l_{12}, then

$$dl_{12} = l_{12} - \left\|\overline{C_1C_2}\right\| = \frac{(C_2 - C_1)^{\mathrm{T}}}{\left\|\overline{C_1C_2}\right\|}(dC_2 - dC_1) \tag{10}$$

For the other two limbs C_1C_3 and C_2C_3, there exists the same relationship

$$\begin{cases} dl_{23} = l_{23} - \frac{(C_3-C_2)^{\mathrm{T}}}{\left\|\overline{C_2C_3}\right\|}(dC_3 - dC_2) \\ dl_{31} = l_{31} - \frac{(C_3-C_1)^{\mathrm{T}}}{\left\|\overline{C_1C_3}\right\|}(dC_3 - dC_1) \end{cases} \tag{11}$$

From equations (10) and (11), the following expression can be obtained

$$d\boldsymbol{\eta_i} = \boldsymbol{J}^{-1}d\boldsymbol{l} \tag{12}$$

where

$$\boldsymbol{J} = \begin{bmatrix} -\frac{(C_2-C_1)^{\mathrm{T}}}{\left\|\overline{C_1C_2}\right\|}\dot{\boldsymbol{C}}_1 & \frac{(C_2-C_1)^{\mathrm{T}}}{\left\|\overline{C_1C_2}\right\|}\dot{\boldsymbol{C}}_2 & 0 \\ 0 & -\frac{(C_3-C_2)^{\mathrm{T}}}{\left\|\overline{C_2C_3}\right\|}\dot{\boldsymbol{C}}_2 & \frac{(C_3-C_2)^{\mathrm{T}}}{\left\|\overline{C_2C_3}\right\|}\dot{\boldsymbol{C}}_3 \\ -\frac{(C_3-C_1)^{\mathrm{T}}}{\left\|\overline{C_1C_3}\right\|}\dot{\boldsymbol{C}}_1 & 0 & \frac{(C_3-C_1)^{\mathrm{T}}}{\left\|\overline{C_1C_3}\right\|}\dot{\boldsymbol{C}}_3 \end{bmatrix},$$
$$\dot{\boldsymbol{C}}_i = \boldsymbol{e}^{\hat{\boldsymbol{u}}_{iO}\theta_i}\boldsymbol{e}^{\hat{\boldsymbol{v}}_{iO}\eta_i}\hat{\boldsymbol{v}}_{iO}\boldsymbol{w}_{iO}$$
$$d\boldsymbol{l} = \begin{bmatrix} l_{12} - \left\|\overline{C_1C_2}\right\| & l_{23} - \left\|\overline{C_2C_3}\right\| & l_{31} - \left\|\overline{C_3C_1}\right\| \end{bmatrix}^{\mathrm{T}}.$$

The matrix $\boldsymbol{J}$ is the Jacobian matrix of 3-RRS SPM. The Jacobian matrix $\boldsymbol{J}$ expresses the mapping relationship between the displacement of the moving platform and the driving angles of 3-RRS SPM when the passive angles η_i ($i = 1, 2, 3$) are used as driving angles.

From equation (12), $d\boldsymbol{\eta_i} = \boldsymbol{J}^{-1}d\boldsymbol{l}$, the iteration equation of $\boldsymbol{\eta} = [\,\eta_1 \quad \eta_2 \quad \eta_3\,]$ can be obtained

$$\boldsymbol{\eta}^{(k+1)} = \boldsymbol{\eta}^{(k)} + (\boldsymbol{J}^{-1}d\boldsymbol{l})^{(k)} \tag{13}$$

where k is the iteration time.

After the passive angles η_i ($i = 1, 2, 3$) are obtained using Newton iteration method, the rotation matrix $\boldsymbol{R}_b^m$ can be obtained using Rodrigues' exponential product equation. Furthermore, the coordinates $\boldsymbol{p}_O$ of center P of the moving platform in the O-XYZ system are obtained as follows

$$\boldsymbol{p}_O = \boldsymbol{R}_b^m\boldsymbol{p} \tag{14}$$

The inverse kinematic analysis of 3-RRS SPM

The inverse position solution is to solve three driving angles ($\theta_1, \theta_2, \theta_3$) for a given orientation (α, β, γ) of the moving platform.

The coordinates of the unit vector $\boldsymbol{w}_i$ ($i = 1, 2, 3$) in the m-xyz system are

$$\begin{bmatrix} \boldsymbol{w}_{1m} \\ \boldsymbol{w}_{2m} \\ \boldsymbol{w}_{3m} \end{bmatrix} = \begin{bmatrix} 1 & 0 & 0 \\ 0 & 1 & 0 \\ 0 & 0 & 1 \end{bmatrix} \tag{15}$$

The vector $\boldsymbol{w}_{im}$ ($i = 1, 2, 3$) can be transformed to the base system O-XYZ using transformation matrix $\boldsymbol{R}_b^m$

$$\boldsymbol{w}_{iO} = \boldsymbol{R}_b^m\boldsymbol{w}_{im}^{\mathrm{T}} \tag{16}$$

that is

$$[\,\boldsymbol{w}_{1O} \quad \boldsymbol{w}_{2O} \quad \boldsymbol{w}_{3O}\,] = \begin{bmatrix} c\alpha c\beta & c\alpha s\beta s\gamma - s\alpha c\gamma & c\alpha s\beta c\gamma + s\alpha s\gamma \\ s\alpha c\beta & s\alpha s\beta s\gamma + c\alpha c\gamma & s\alpha s\beta c\gamma - c\alpha s\gamma \\ -s\beta & c\beta s\gamma & c\beta c\gamma \end{bmatrix}$$

When the angles α, β, and γ are known in the transformation matrix $\boldsymbol{R}_b^m$, the unit vectors $\boldsymbol{v}_i$ and vectors $\boldsymbol{w}_i$ are connected by the coupler in each limb. The dimensional angle of link B_iC_i is δ_2. This relationship can be used to establish the constraint equation as follows

$$\boldsymbol{v}_i \cdot \boldsymbol{w}_i = \cos\ \delta_2 (i = 1, 2, 3) \tag{17}$$

that is

$$v_{iox}w_{iox} + v_{ioy}w_{ioy} + v_{ioz}w_{ioz} = \cos\ \delta_2 \tag{18}$$

The constraint equations of 3-RRS SPM are as follows

$$\begin{cases} c\delta_2 = c\delta_1 c\alpha c\beta - s\delta_1 s\beta s\theta_1 + s\delta_1 s\alpha c\beta c\theta_1 \\ c\delta_2 = (s\alpha s\beta s\gamma + c\alpha c\gamma)c\delta_1 + (c\alpha s\beta s\gamma - s\alpha c\gamma)s\delta_1 s\theta_2 \\ \quad + c\beta s\gamma s\delta_1 c\theta_2 \\ c\delta_2 = c\delta_1 c\beta c\gamma + (s\alpha s\beta c\gamma - c\alpha s\gamma)s\delta_1 s\theta_3 \\ \quad + (c\alpha s\beta c\gamma + s\alpha s\gamma)s\delta_1 c\theta_3 \end{cases} \tag{19}$$

Equation (19) yields

$$D_i\ \sin\ \theta_i + E_i\ \cos\ \theta_i = F_i (i = 1, 2, 3) \tag{20}$$

where

$$\begin{cases} D_1 = -s\delta_1 s\beta \\ E_1 = s\delta_1 s\alpha c\beta \\ F_1 = c\delta_2 - c\delta_1 c\alpha c\beta \end{cases}, \begin{cases} D_2 = (c\alpha s\beta s\gamma - s\alpha c\gamma)s\delta_1 \\ E_2 = c\beta s\gamma \sin\delta_1 \\ F_2 = c\delta_2 - (s\alpha s\beta s\gamma + c\alpha c\gamma)c\delta_1 \end{cases},$$

$$\begin{cases} D_3 = (s\alpha s\beta c\gamma - c\alpha s\gamma)s\delta_1 \\ E_3 = (c\alpha s\beta c\gamma + s\alpha s\gamma)s\delta_1 . \\ F_3 = c\delta_2 - c\delta_1 c\beta c\gamma \end{cases}$$

Equation (20) is a first-order equation about $\sin\ \theta_i$ and $\cos\ \theta_i$.

Let $\tan(\theta_i/2) = t_i$, then $\begin{cases} \sin\ \theta_i = (2t_i)/(1 + t_i^2) \\ \cos\ \theta_i = (1 - t_i^2)/(1 + t_i^2) \end{cases}$.

Substituting it into equation (20) yields

$$(E_i + F_i)t_i^2 - 2D_it_i - E_i + F_i = 0 (i = 1, 2, 3) \tag{21}$$

Thus

$$t_i = \frac{D_i \pm \sqrt{D_i^2 + E_i^2 - F_i^2}}{(E_i + F_i)} (i = 1, 2, 3) \tag{22}$$

Therefore, the inverse position solution of 3-RRS SPM is obtained as follows

$$\theta_i = 2\ \arctan\left(\frac{D_i \pm \sqrt{D_i^2 + E_i^2 - F_i^2}}{(E_i + F_i)}\right) (i = 1, 2, 3) \tag{23}$$

θ_i has two solutions for limb i. This shows that the inverse position solutions have eight sets of solutions for a given position and orientation of 3-RRS SPM.

Case study

The structure parameters of 3-RRS SPM are shown in Table 3. Figure 7 is the simulation model of 3-RRS SPM.

The moving platform and the base of 3-RRS SPM are parallel to each other when 3-RRS SPM is located in the initial position. When the driving angles $\theta_1 = -30°$, $\theta_2 = -45°$, and $\theta_3 = -45°$, the forward kinematics leads to $\boldsymbol{\eta} = [\,0.1 \quad 0.2 \quad 0.4\,]$, the transformation matrix $\boldsymbol{R}_b^m$ is further obtained

Table 3. The structure parameters of 3-RRS SPM.

δ_1 (°)	δ_2 (°)	φ_1 (°)	φ_2 (°)	r (mm)
45	45	54.74	54.74	60
r_b (mm)	r_c (mm)	h_1 (mm)	h_2 (mm)	l_s (mm)
54	41	2	2	5

Table 4.The results of the inverse position solutions of 3-RRS SPM.

No.	θ_1 (°)	θ_2 (°)	θ_3 (°)
1	145.92	126.87	118.68
2	−30.02	−44.99	−44.99

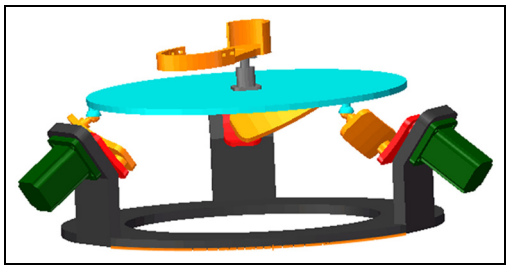

Figure 7. The simulation model of 3-RRS SPM.

$$\boldsymbol{R}_b^m = \begin{bmatrix} 0.9975 & 0.1064 & 0.1668 \\ 0.0599 & 0.9900 & 0.2226 \\ 0.0375 & 0.0923 & 0.9605 \end{bmatrix} \quad (24)$$

The values of the driving angles can be obtained as shown in Table 4 using inverse position solution equations and substituting the structure parameters in Table 3 and the value of transformation matrix $\boldsymbol{R}_b^m$ in equation (24). To sum up, the driving angles (θ_1, θ_2, θ_3) have eight kinds of combination for a given position and orientation of the moving platform.

Observing Table 4, the second sets of the inverse position solutions, that is, $\theta_1 = -30.02°$, $\theta_2 = -44.99°$, and $\theta_3 = -44.99°$, are the same as the driving angles $\theta_1 = -30°$, $\theta_2 = -45°$, and $\theta_3 = -45°$ within the range of acceptable errors. This verifies the inverse position solutions of 3-RRS SPM.

Conclusion

This article proposes a new ankle rehabilitation robot based on 3-RRS SPM, which accords with the topology structure of ankle. 3-RRS SPM can move along a spherical trajectory in the space, and therefore, it can realize the motion of ankle.

The kinematics of 3-RRS SPM is analyzed. Eight sets of inverse kinematics are obtained. The case verifies the inverse position solutions of 3-RRS SPM.

The ankle rehabilitation robot has a high potential for rehabilitation applications; it can be widely used in clinical treatment and can also be used at home, hotels, and fitness centers for ankle muscle relaxation.

Declaration of conflicting interests

The author(s) declared no potential conflicts of interest with respect to the research, authorship, and/or publication of this article.

Funding

The author(s) disclosed receipt of the following financial support for the research, authorship, and/or publication of this article: The work was partially funded by the National Natural Science Foundation of China (grant no. 51275486).

References

1. David BT. *Foot & ankle (orthopaedic surgery essentials)*. 2nd ed. Philadelphia, PA: Lippincott Williams & Wilkins, 2013.
2. Bian H, Liu YH, Liang ZC, et al. A novel 2-RRR/UPRR robot mechanism for ankle rehabilitation and its kinematics. *Robot* 2010; 32: 6–12 (in Chinese).
3. Wang YF, Mei ZY, Xu JL, et al. Kinematic design of a parallel ankle rehabilitation robot for sprained ankle physiotherapy. In: *Proceedings of the 2012 IEEE international conference on robotics and biomimetics*, Guangzhou, China, 11–14 December 2012. New York: IEEE.
4. Shah MN and Basah SN. Design and kinematic analysis of parallel robot for ankle rehabilitation. *Appl Mech Mater* 2014; 446–447: 1279–1284.
5. Hou YP, Ceng XF and Xu Q. The mechanism research for ankle rehabilitation. *J Hebei United Univ* 2013; 35: 55–58 (in Chinese).
6. Zeng DX, Hu ZT, Hou YL, et al. Novel decoupled parallel mechanism for ankle rehabilitation and its optimization. *J Mech Eng* 2015; 51: 1–9 (in Chinese).
7. Jamwal PK, Xie SQ and Aw KC. Kinematic design optimization of a parallel ankle rehabilitation robot using modified genetic algorithm. *Robot Auton Syst* 2009; 57: 1018–1027.
8. Dai JS, Zhao TS and Nester C. Sprained ankle physiotherapy based mechanism synthesis and stiffness analysis of a robotic rehabilitation device. *Auton Robot* 2004; 16: 207–218.
9. Girone M, Burdea G, Bouzit M, et al. A Stewart platform-based system for ankle telerehabilitation. *Auton Robot* 2001; 10: 203–212.
10. Zhao TS, Dai JS and Huang Z. Geometric analysis of overconstrained parallel manipulators with three and

four degrees of freedom. *J Soc Mech Eng* 2002; 45: 730–740.
11. Kapandji AI. *The physiology of the joint: Volume 2 Lower limb*. 6th ed. London: Churchill Livingstone, 2010.
12. Paley D. *Principles of deformity correction*. Berlin: Springer, 2002.
13. Yao TS and Meng XJ. *Ankle surgery*. Beijing, China: Press of Traditional Chinese Medicine, 1998 (in Chinese).
14. Zhang Y. *Research and development on ankle-foot rehabilitation exoskeleton orthosis*. MSc Thesis, Zhejiang University, Hangzhou, China, 2010.
15. Bai S, Hansen MR and Angeles J. A robust forward-displacement analysis of spherical parallel robots. *Mech Mach Theory* 2009; 44: 2204–2216.
16. Bai S. Optimum design of spherical parallel manipulators for a prescribed workspace. *Mech Mach Theory* 2010; 45: 200–211.